Novel strontium-doped bioactive glass nanoparticles enhance proliferation and osteogenic differentiation of human bone marrow stromal cells

Strobel, L A ; Hild, N ; Mohn, D ; Stark, W J ; Hoppe, A ; Gbureck, U ; Horch, R E ; Kneser, U ; Boccaccini, A R

DOI: https://doi.org/10.1007/s11051-013-1780-5

Novel strontium-doped bioactive glass nanoparticles enhance proliferation and osteogenic differentiation of human bone marrow stromal cells

L. A. Strobel[1,2]; N. Hild[3], D. Mohn[3,4]; W. J. Stark[3]; A. Hoppe[5]; U. Gbureck[6]; R. E. Horch[1]; U. Kneser[1,2] ; A. R. Boccaccini[5]*

[1] Department of Plastic and Hand Surgery, University of Erlangen-Nuremberg Medical Center, Erlangen, Germany

[2] Department of Hand, Plastic and Reconstructive Surgery, Burn Centre, BG Trauma Centre, Ludwigshafen/Rhine, Germany

[3] Institute for Chemical and Bioengineering, Department of Chemistry and Applied Biosciences, ETH Zurich, Zurich, Switzerland

[4] Department of Preventive Dentistry, Periodontology and Cariology, University of Zurich, Center of Dental Medicine, Zurich, Switzerland

[5] Institute of Biomaterials, University of Erlangen-Nuremberg, Erlangen, Germany

[6] Department for Functional Materials in Medicine and Dentistry, University of Würzburg, Würzburg, Germany

*Correspondence to:

Prof. Dr.-Ing. habil. Aldo R. Boccaccini

Institute of Biomaterials

Department of Materials Science and Engineering

University of Erlangen-Nuremberg

Cauerstrasse 6

91058 Erlangen, Germany

Tel.: +49 9131 85 28601

Fax: +49 9131 85 28602

Email: aldo.boccaccini@ww.uni-erlangen.de

Abstract

The present study investigates a new family of bioactive glass nanoparticles with and without Sr doping focusing on the influence of the nanoparticles on human bone marrow stromal cells (hBMSCs) *in vitro*. The bioactive glass nanoparticles were fabricated by flame spray synthesis and a particle diameter of 30 to 35 nm was achieved. Glass nanoparticles were undoped (BG 13-93-0Sr) or doped with 5 wt.-% strontium (Sr) (BG 13-93-5Sr) and used at concentrations of 10 µg/cm² and 100 µg/cm² (particles per culture plate area), respectively. Cells were cultured for 14 days after which the samples were analysed regarding metabolic activity and expression of various bone-specific genes. Cell growth and morphology indicated the high cytocompatibility of the nanoparticulate bioactive glass. The presence of the nanoparticles enhanced cell growth compared to the plain polystyrene control group. At a concentration of 100 µg/cm², Sr-doped particles led to significantly enhanced gene expression of osteocalcin, collagen type 1 and vascular endothelial growth factor (VEGF). Thus Sr-doped nanoparticles showing a dose-dependent increase of osteogenic differentiation in hBMSCs are a promising biomaterial for bone regeneration purposes.

Key words

Bioactive glass, human bone marrow stromal cells, nanoparticles, osteogenic differentiation, strontium, bone tissue engineering

1. Introduction

Bioactive glasses are widely used in the field of regenerative medicine due to their high bone bonding ability and their osteogenic potential (Hench and Polak 2002; Hoppe et al. 2011). Ionic dissolution products released from bioactive glasses are known to stimulate several osteogenesis related genes (Hench 1998; Hoppe et al. 2011). Recently, novel approaches have been proposed in order to enhance the biocompatibility of bioactive glasses by adding bioactive metal ions to the glass network (Hoppe et al. 2011). Among many therapeutically active metals and inorganic ions, strontium (Sr) ions are known to have beneficial effects on bone cells and *in vivo* bone formation, the latter make them highly attractive agents for bone tissue engineering applications (Marie et al. 2001). Dissolution products from bioactive glasses doped with Sr have been shown to enhance osteogenic differentiation of human osteosarcoma cells (SaOS-2) and also to reduce osteoclast activity, hence, affecting bone turn over (Gentleman et al. 2010a).

There is recent interest in investigating bioactive glass nanoparticles for bone regeneration due to their potential higher biological reactivity compared with conventional (μm- sized) particles (Misra et al. 2008). Indeed nanoscaled bioactive glass particles have been shown to offer several advantages over micron sized particles, such as improved mechanical properties when used as filler materials in biocomposites (Boccaccini et al. 2010) or enhanced *in vitro* bioactivity (Misra et al. 2008, Mackovic et al. 2012). Nanoparticulate bioactive glasses with a chemical structure that is similar to Hench's 45S5 composition (Hench 1998) also display antibacterial properties and have potential for dentin remineralisation when applied to demineralised dentin matrix (Curtis et al. 2010; Vollenweider et al. 2007; Waltimo et al. 2007). Labbaf

et al investigated sub-micron bioactive glass particles of composition 85 mol% SiO_2 and 15 mol% CaO, synthesised by the sol-gel process, confirming the non-toxicity of the sub-micron bioactive glass particles (Labbaf et al. 2011). It is thus of high interest to develop and investigate bioactive glass nanoparticles with different chemical composition.

Flame spray synthesis, a scalable and cost efficient process to produce inorganic nanoparticles (Stark and Pratsinis, 2002, Teoh et al. 2010), was used in the present work for the first time to synthesize a new family of glass nanoparticles containing 7 different components (SiO_2, Na_2O, P_2O_5, K_2O, MgO, CaO and SrO). To the authors' knowledge, there is no other technique that allows for synthesizing this kind of multicomponent nanoparticulate bioactive glass. Furthermore, this method guarantees narrow particle size distribution in addition to the low risk of product contamination (Brunner et al., 2006, Teoh et al., 2010).

The aim of this study was thus to assess the osteogenic potential of a new family of bioactive glass nanoparticles containing Sr and to unveil possible stimulating effects of Sr ions on human bone marrow stromal cells (hBMSCs). Detailed gene expression profile of these cells will be used to determine any specific effects of Sr on osteogenic differentiation.

2. Materials and Methods

2.1 Material preparation and characterisation

The nanoparticulate glasses were produced via a one step and dry synthesis method in a flame aerosol reactor described in detail by Brunner *et al* (Brunner et al. 2006). In

brief, the corresponding metal precursors of Si (hexamethyldisiloxane, ABCR), Na (sodium hydroxide dissolved in 2-ethylhexanoic acid, Sigma Aldrich), P (tributylphosphate, Acros Organics), K (potassium bicarbonate dissolved in 2-ethylhexanoic acid, Sigma Aldrich), Mg (magnesium oxide dissolved in 2-ethylhexanoic acid, Sigma Aldrich), Ca (calcium hydroxide dissolved in 2-ethylhexanoic acid, Sigma Aldrich) and Sr (strontium acetate dissolved in 2-ethylhexanoic acid, Sigma Aldrich) were mixed according to the final glass composition, as shown in Table 1, and diluted with xylene (technical grade). The solution was fed (5 ml/min) through a nozzle, dispersed by oxygen (5 l/min) and ignited with a preflame (methane/oxygen 1.13/2.4 l/min). Particles formed during burning of the precursor were collected on a fibre filter mounted above the flame (40 cm). Collected particles were sieved (150 µm) and characterised subsequently.

The specific surface area (SSA) of the nanoparticles was measured using the Brunauer-Emmet-Teller (BET) method at 77 K on a Tristar instrument (Micromeritics, Norcross, GA, USA). Particle shape was determined with transmission electron microscopy (TEM) on a Tecnai F30 ST (FEI, FEG, 300 kV). X-ray diffraction (XRD) patterns were recorded on a X'Pert PRO-MPD diffractometer (Cu-K_α radiation, X'Celerator linear detector system, PANalytical, Netherlands) with a step size of 0.033°.

For cell culture, bioactive glass nanoparticles were sterilised by dry heat at 180°C for 2 h in a furnace. Afterwards the particles were dispersed in an ultrasonic bath (Sonorex RK102M; f=50-60Hz, Bandelin electronic, Berlin, Germany) in serum-free medium for 30 minutes. Fetal bovine serum (FBS) was added prior to cell contact.

2.2 Cell culture

The hBMSCs were purchased from PromoCell (hMSC-BM, Catalogue number C-12975, PromoCell Heidelberg, Germany). Cells were cultured in flasks (COSTAR, Cambridge, USA) in an incubator (at 37 ºC and 5% CO_2) and used at passage 5. The culture medium was used as DMEM/Ham's F-12 (1:1) with 10% FBS, 1% penicillin-streptomycin and 2 mg/l L-glutamine (all from Biochrom AG, Berlin, Germany). The medium was changed twice a week. At 80-90% confluency level cells were trypsinised (Trypsin EDTA, PAA, Pasching, Austria) and cultured further. After cell expansion, cells of passage 6 were used for the experiment. **Cell morphology**, growth and viability were observed over time by light microscopy (Leica DM IL, Leica, Wetzlar, Germany).

2.3 Experimental design

Five different groups were evaluated in this study. For the control group, hBMSCs were cultured on plain tissue culture polystyrene (well plates without glass particles). In addition, nanoparticulate glass without Sr (BG 13-93-0Sr) and Sr-doped nanoparticulate glass (BG 13-93-5Sr) were used each in two different concentrations, 10 µg/cm² and 100 µg/cm² (particles per culture plate area). For light microscopic observations of cell culture an additional concentration of 1 µg/ml of each bioactive glass was included. Medium containing dispersed nanoparticulate glass was added and 50 000 hBMSCs/well were seeded in 6-well plates (Cellstar®, Greiner Bio-One, Frickenhausen, Germany). The initial concentration of nanoparticles was each 2.4 µg/ml (in groups with 10 µg/cm²) and 24 µg/ml (in groups with 100 µg/cm²) in 4 ml of total cell culture medium. Only the upper half of medium was changed twice a week to ensure glass nanoparticles remaining at the bottom of the wells.

2.4 ICP-MS analysis

To measure Sr ions in the cell culture media and to detect differences in Sr-release between the experimental groups, the media were collected, pooled (6 independent samples) and used for analysis. Sr levels were quantified by inductively coupled plasma-mass spectroscopy (ICP-MS, Varian, Darmstadt, Germany) against standard solutions of 50 and 100 µg/l according to manufacturer's instructions.

2.5 Cell metabolic activity

Metabolic activity of hBMSCs was analysed by AlamarBlue assay (Biosource Int., Camarillo, CA USA) after 14 days. The medium was aspirated and 1.5 ml of culture medium containing 10% AlamarBlue was added. After incubation for 3 hours at 37°C, absorbance was measured using a plate reader (SPECTRAmax 190, Molecular Devices, Sunnyvale, CA USA) at 570 nm and 600 nm. The percentage of AlamarBlue reduction was calculated according to manufacturer's recommendations.

2.6 Molecular analysis

Cells for RNA isolation were detached (2 wells/sample) in triplicate with 1 ml of TRIzol Reagent (Invitrogen, Carlsbad, CA, US) and vortexed with 200 µl of Chloroform (Sigma-Aldrich, Steinheim, Germany). Total RNA was isolated using RNeasy Mini Kit (Qiagen, Hilden, Germany) according to manufacturer's instructions. RNA (1 mg) from each sample was reverse transcribed into complementary DNA using QuantiTect Reverse Transcription Kit (Qiagen, Hilden, Germany) according to manufacturer's recommendations.

Real-time reverse transcription polymerase chain reaction (RT-PCR) was performed with selected primer sequences as shown in Table 2. The expression of

glyceraldehyde-3-phosphate dehydrogenase (GAPDH), osteocalcin, collagen type 1, vascular endothelial growth factor (VEGF) and Runt-related transcription factor 2 (Runx2) was quantified using QuantiTect SYBR Green PCR Kit (iQ SYBR green, Bio-Rad Laboratories, Hercules, CA USA). GAPDH was used as reference. Results were calculated using relative quantification (ΔΔCt method) compared to the control group. Every sample was analysed in duplicate. Results are expressed as fold changes of the expression of each gene in relation to the control group at each time point.

2.7 Statistical analysis

Results are given as mean ± standard error of the mean (SEM). A one-way analysis of variance (ANOVA) and Bonferroni's multiple comparison posthoc test was used to compare various groups. P-values < 0.05 are considered as statistically significant.

3. Results and discussion

3.1 Electron microscopy

TEM images revealed nanometric spherical particles that showed interconnectivity between the spheres whilst having an XRD-amorphous nature (Figure 1 and supplementary data). This behaviour is regularly observed for bioactive glass particles in the nanometric size range even if more oxides were present than for the classical 45S5 Bioglass® (Mohn et al. 2010). The SSA of all as-prepared particles was in the same range and confirmed the nanoscale of the particles (Table 1).

3.2 Strontium dissolution assay

Amounts of Sr ions in cell culture media were detected by ICP-MS analysis after 2 weeks (Figure 2A). There was a basal amount of Sr (22 µg/l) in the control culture

medium attributable to the serum. The same basal Sr level was found in the media of groups with Sr-free (BG 13-93-0Sr) bioactive glass. The highest amount of Sr was measured in the culture medium of the group containing 100 µg/cm² Sr-doped nanoparticulate glass (BG 13-93-5Sr). Of course, it was impossible to avoid some Sr ions getting lost by media changes over time. However, ICP analyses confirmed that Sr-doped nanoparticles led to critical Sr levels in culture medium even after 2 weeks. Sr levels were 77.01 µg/l for samples with 10 µg/cm² Sr-doped particles and 480.30 µg/l in samples with 100 µg/cm² Sr-doped particles. A continuous effect of Sr on the cells can consequently be assumed. Lao *et al* investigated the release of Sr in DMEM using Sr-doped mesoporous bioactive glass discs and particles (0, 1, 5 wt.-%) (Lao et al. 2008). After 10 days of interaction, the measured Sr concentrations were similar to concentrations in plasma of animals treated with Sr-based drugs showing anti-osteoporotic effects (Dahl et al. 2001). Additionally, influences of Sr on bioactive glasses were found, such as induced and accelerated formation of surface bone-like apatite layers and reduced dissolution of the mesoporous glasses (Lao et al. 2008). Recently, Wu *et al* used periodontal ligament cells (PDLCs) to investigate the effect of Sr-incorporation in mesoporous bioactive glass scaffolds and showed increased ALP activity and cementogenic gene expression (Wu et al. 2012). *In vivo* studies with different bioactive glasses containing Sr have shown biocompatibility, osteoconductivity and bone formation, offering advantages also in osteoporotic animals (Boyd et al. 2009; Gorustovich et al. 2010b). These observations are indicative that the currently used materials encourage cell adhesion and provide a certain degree of bone healing capacity even without exhibiting a nanostructure. In the present study, it was possible to

optimise potential bone formation properties by combining the advantages of bioactive glass and Sr-release with the nanoscale dimension of the particles used. Further experiments with Sr-doped nanoparticles to investigate the influence of Sr on bioactivity as well as Sr-release kinetics and to develop controlled Sr-releasing systems are thus justified following the present results.

3.3 Cell proliferation and metabolic activity

Cell morphology and viability were observed in every group by light microscopy over time. After 14 days of culture the common spindle-like morphology of viable hBMSCs was observed as shown in Figure 3. At this time an adequate number of cells were achieved in the well plate. There were no indications of cytotoxic effects of the material or infections. Due to the low magnification of the lightmicroscopic picture, nanoparticles are not visible in Figure 3. Nevertheless, evaluation of the effects of nanoparticles show that the cell growth is increased by a higher concentration of nanoparticles. The presence of Sr seems to have no appreciable influence on cell morphology and interaction of hBMSCs.

After 14 days, AlamarBlue analysis confirmed the microscopic observations regarding cell proliferation. Metabolic activity of hBMSCs was significantly enhanced in both groups containing 100 µg/cm² nanoparticulate glass compared to the control group (Figure 2B). In the current experiment, no influence of Sr on metabolic activity of hBMSCs could be detected (no statistical significance between BG 13-93-0Sr and BG 13-93-5Sr groups).

While plenty is known about the effect of growth factors and cytokines on hBMSCs, there still is a lack of information regarding physical and chemical extracellular conditions regulating proliferation and differentiation of bone cells. Nanostructures imitate the extracellular matrix of natural bone. These structures are supposed to improve bone cell adhesion due to high porosity as well as high surface area-to-volume-ratio (Lim et al. 2011). Besides, ionic dissolution products of bioactive glasses are known to stimulate the growth of human osteoblasts (Sun et al. 2007). In this study,

both nanoparticulate glasses were proved to be cytocompatible and non-toxic. Indeed, metabolic activity of hBMSCs could be significantly enhanced by merging the advantages of bioactive glasses and nanoscaled particles. Consistent with our above-mentioned findings, it has been described previously that Sr-incorporation in bioactive glass has no influence on osteoblastic cell growth at an early culture time (after 2 and 4 days of cultivation) (Isaac et al. 2011). Furthermore, Sila-Asna *et al* reported that Sr-containing cell culture medium does not affect the proliferation of hBMSCs up to 18 days and enhances proliferation only after 21 days of interaction (Sila-Asna et al. 2007).

3.4 Quantitative real-time RT-PCR

To investigate the osteogenic differentiation of hBMSCs, bone specific gene expression was detected after 14 days. Cells grown on polystyrene (without nanoparticulate bioactive glass) served as control. The expression of osteocalcin and collagen type 1 was significantly up-regulated in cells cultured in presence of 100 µg/cm² Sr-doped nanoparticles compared to all other groups (**Figure 4**). These results show a strong enhancement of bone-specific genes due to Sr-containing bioactive glass without any osteoinductive medium supplements.

The two main types of proteins in the extracellular matrix of bone are collagens (mainly collagen type 1) and the noncollagenous proteins, for example osteocalcin. Osteocalcin is known as the most specific protein for osteogenic matrix maturation. It is found in post-mitotic mature osteoblasts (Aubin et al. 1995). Moreover, Runx2 is indicative of osteoblast differentiation, as it is a key transcription factor for up-regulation of osteocalcin, collagen type 1 and other bone-specific genes. The extent of collagen type 1 expression and Runx2 expression in the samples correlated well with the osteocalcin-

expression (Figure 4). VEGF is known to enhance angiogenic properties in various cell types including induced expression of certain microRNAs that enhance CD34+ stem cell function (Alaiti et al. 2012). This analysis shows that not only osteogenic but also the angiogenic marker VEGF is up-regulated by Sr-doped nanoparticles providing attractive properties for bone regeneration. Moreover, cells cultured in presence of both types of nanoparticulate glasses showed slightly enhanced bone-specific gene expression patterns compared to the control group. Nevertheless, this finding is not statistically significant in the current experimental setting. This result may be due to the limited sample size and the fixed time of analysis. Bioactive glasses have attracted much attention in bone tissue engineering because of their osteogenic properties (Gentleman et al. 2010b; Hoppe et al. 2011; Sun et al. 2007). The released ionic dissolution products are capable of enhancing proliferation and differentiation of bone cells and inducing angiogenesis (Gorustovich et al. 2010a; Hoppe et al. 2011; Xynos et al. 2000).

It has already been shown that Sr promotes osteogenic differentiation of bone cells through different signalling pathways (Peng et al. 2009; Yang et al. 2011). Briefly, Sr enhances bone formation by inhibition of osteoclasts and stimulation of osteoblasts (Marie et al. 2001). Isaac *et al* demonstrated enhanced osteogenic properties due to Sr-doping of bioactive glasses (Isaac et al. 2011). Moreover, hydroxyapatite (HAP) nanoparticles that were Sr-doped resulted in higher osteoconductive and osteoinductive behaviour in comparison to Sr-free particles, as reported in a very recent study (Hao et al. 2012).

Based on our observations, the present nanoparticles possess high biological activity and osteogenic properties which are attributed to the benefit of both the Sr-doping and

nanostructured surface. A dose-dependent stimulating effect of Sr-doped nanoparticulate glass on osteogenic cells can be assumed. In addition to optimisation of biomaterial composition and properties, adequate cell sources are required for successful bone regeneration. hBMSCs are commonly used in bone tissue engineering showing well-known characteristics of stem cells such as self-renewal, multipotency and high potential for *ex vivo* expansion. Especially in the rapid developing field of "nano-regenerative medicine", hBMSCs seem to be a favourable cell source (Arora et al. 2012).

Regarding standard *in vivo* models for bone tissue engineering purposes, Sr-doped bioactive glass nanoparticles could be applied in many different ways. For instance, particles could be used as add-on to cell suspensions or as a surface coating on three-dimensional bone substitutes. So the bioactive glass nanoparticles used in this study provide high potential to become a therapeutic option for bone tissue engineering applications and should be analysed in standard *in vivo* models.

4. Conclusions

The present study introduces a novel Sr-doped nanostructured bioactive glass with primary particle diameters in the range of 30-35 nm. This nanoscale biomaterial might promote osteogenic and angiogenic properties of hBMSCs. Cell metabolic activity was found to be independent of Sr, but increased in presence of nanoparticulate glass. hBMSCs that were cultured in presence of the Sr-doped nanoparticles developed a significant upregulation of osteocalcin, collagen type 1 and VEGF. These findings indicate that the currently described Sr-doped nanostructured glass combines the Sr-

induced osteogenic stimulation with the advantageous properties of nanostructures and bioactive glasses. Our observations provide the basis for further studies with regard to Sr-delivering nanostructured glasses for bone tissue engineering applications.

Acknowledgements

This work was partially supported by the Emerging Fields Initiative (EFI) of the University of Erlangen-Nuremberg, Germany (project “TOPbiomat”) and a research grant from the Deutsche Forschungsgemeinschaft DFG (KN 578/2-1). The authors gratefully thank Marina Milde for expert technical assistance.

Disclosures

None of the authors has any financial interest to declare in relation to the content of this article.

References

Alaiti MA, Ishikawa M, Masuda H, Simon DI, Jain MK, Asahara T, Costa MA (2012) Up-Regulation of miR-210 by Vascular Endothelial Growth Factor in Ex Vivo Expanded CD34+ Cells Enhances Cell-Mediated Angiogenesis. J Cell Mol Med

Arora P, Sindhu A, Dilbaghi N, Chaudhury A, Rajakumar G, Rahuman AA (2012) Nano-regenerative medicine towards clinical outcome of stem cell and tissue engineering in humans. J Cell Mol Med

Aubin JE, Liu F, Malaval L, Gupta AK (1995) Osteoblast and chondroblast differentiation. Bone 17:77S-83

Boccaccini AR, Erol M, Stark WJ, Mohn D, Hong Z, Mano JF (2010) Polymer/bioactive glass nanocomposites for biomedical applications: A review. Composites Science and Technology 70:1764-1776

Boyd D, Carroll G, Towler MR, Freeman C, Farthing P, Brook IM (2009) Preliminary investigation of novel bone graft substitutes based on strontium-calcium-zinc-silicate glasses. J Mater Sci Mater Med 20:413-20

Brunner TJ, Grass RN, Stark WJ (2006) Glass and bioglass nanopowders by flame synthesis. Chemical Communications:1384-1386

Curtis AR, West NX, Su B (2010) Synthesis of nanobioglass and formation of apatite rods to occlude exposed dentine tubules and eliminate hypersensitivity. Acta Biomaterialia 6:3740-3746

Dahl SG, Allain P, Marie PJ, Mauras Y, Boivin G, Ammann P, Tsouderos Y, Delmas PD, Christiansen C (2001) Incorporation and distribution of strontium in bone. Bone 28:446-53

Gentleman E, Fredholm YC, Jell G, Lotfibakhshaiesh N, O'Donnell MD, Hill RG, Stevens MM (2010) The effects of strontium-substituted bioactive glasses on osteoblasts and osteoclasts in vitro. Biomaterials 31:3949-3956

Gorustovich AA, Roether JA, Boccaccini AR (2010a) Effect of bioactive glasses on angiogenesis: a review of in vitro and in vivo evidences. Tissue Eng Part B Rev 16:199-207

Gorustovich AA, Steimetz T, Cabrini RL, Porto Lopez JM (2010b) Osteoconductivity of strontium-doped bioactive glass particles: a histomorphometric study in rats. J Biomed Mater Res A 92:232-7

Hao Y, Yan H, Wang X, Zhu B, Ning C, Ge S (2012) Evaluation of osteoinduction and proliferation on nano-Sr-HAP: a novel orthopedic biomaterial for bone tissue regeneration. J Nanosci Nanotechnol 12:207-12

Hench L (1998) Bioceramics. J Am Ceram Soc 81:1705-61

Hench L, Polak JM (2002) Third-generation biomedical materials. Science 295:1014-7

Hoppe A, Guldal NS, Boccaccini AR (2011) A review of the biological response to ionic dissolution products from bioactive glasses and glass-ceramics. Biomaterials 32:2757-74

Isaac J, Nohra J, Lao J, Jallot E, Nedelec JM, Berdal A, Sautier JM (2011) Effects of strontium-doped bioactive glass on the differentiation of cultured osteogenic cells. Eur Cell Mater 21:130-43

Labbaf S, Tsigkou O, Müller KH, Stevens MM, Porter AE, Jones JR (2011) Spherical bioactive glass particles and their interaction with human mesenchymal stem cells in vitro. Biomaterials 32:1010-1018

Lao J, Jallot E, Nedelec JM (2008) Strontium-Delivering Glasses with Enhanced Bioactivity: A New Biomaterial for Antiosteoporotic Applications? Chem Mater 20:4969-4973

Lim JY, Loiselle AE, Lee JS, Zhang Y, Salvi JD, Donahue HJ (2011) Optimizing the osteogenic potential of adult stem cells for skeletal regeneration. J Orthop Res 29:1627-33

Mačković M, Hoppe A, Detsch R, Mohn D, Stark WJ, Spiecker E, Boccaccini AR (2012) Bioactive glass (type 45S5) nanoparticles: in vitro reactivity on nanoscale and biocompatibility. J. Nanopart. Res. 14:966

Marie PJ, Ammann P, Boivin G, Rey C (2001) Mechanisms of action and therapeutic potential of strontium in bone. Calcif Tissue Int 69:121-9

Misra SK, Mohn D, Brunner TJ, Stark WJ, Philip SE, Roy I, Salih V, Knowles JC, Boccaccini AR (2008) Comparison of nanoscale and microscale bioactive glass on the properties of P(3HB)/Bioglass composites. Biomaterials 29:1750-61

Mohn D, Bruhin C, Luechinger NA, Stark WJ, Imfeld T, Zehnder M (2010) Composites made of flame-sprayed bioactive glass 45S5 and polymers: bioactivity and immediate sealing properties. International Endodontic Journal 43:1037-1046

Peng S, Zhou G, Luk KD, Cheung KM, Li Z, Lam WM, Zhou Z, Lu WW (2009) Strontium promotes osteogenic differentiation of mesenchymal stem cells through the Ras/MAPK signaling pathway. Cell Physiol Biochem 23:165-74

Sila-Asna M, Bunyaratvej A, Maeda S, Kitaguchi H, Bunyaratavej N (2007) Osteoblast differentiation and bone formation gene expression in strontium-inducing bone marrow mesenchymal stem cell. Kobe J Med Sci 53:25-35

Stark WJ, Pratsinis SE (2002) Aerosol flame reactors for manufacture of nanoparticles Powder Technology 126: 103-108

Sun JY, Yang YS, Zhong J, Greenspan DC (2007) The effect of the ionic products of Bioglass dissolution on human osteoblasts growth cycle in vitro. J Tissue Eng Regen Med 1:281-6

Teoh WY, Amal R, Mädler L (2010) Flame spray pyrolysis: An enabling technology for nanoparticles design and fabrication. Nanoscale, 2: 1324-1347

Vollenweider M, Brunner TJ, Knecht S, Grass RN, Zehnder M, Imfeld T, Stark WJ (2007) Remineralization of human dentin using ultrafine bioactive glass particles. Acta Biomaterialia 3:936-943

Waltimo T, Brunner TJ, Vollenweider M, Stark WJ, Zehnder M (2007) Antimicrobial effect of nanometric bioactive glass 45S5. J Dent Res 86:754-7

Wu C, Zhou Y, Lin C, Chang J, Xiao Y (2012) Strontium-containing mesoporous bioactive glass scaffolds with improved osteogenic/cementogenic differentiation of periodontal ligament cells for periodontal tissue engineering. Acta Biomater 8:3805-15

Xynos ID, Edgar AJ, Buttery LD, Hench LL, Polak JM (2000) Ionic products of bioactive glass dissolution increase proliferation of human osteoblasts and induce insulin-like growth factor II mRNA expression and protein synthesis. Biochem Biophys Res Commun 276:461-5

Yang F, Yang D, Tu J, Zheng Q, Cai L, Wang L (2011) Strontium enhances osteogenic differentiation of mesenchymal stem cells and in vivo bone formation by activating Wnt/catenin signaling. Stem Cells 29:981-91

Table 1. Compositions of bioactive glass nanoparticels used.

	SiO_2 [wt%]	Na_2O [wt%]	P_2O_5 [wt%]	K_2O [wt%]	MgO [wt%]	CaO [wt%]	SrO [wt%]	SSA[a] [m^2/g]	d_{BET}[b] [nm]
BG 13-93-0Sr	53	6	4	12	5	20	0	69	34
BG 13-93-5Sr	53	6	4	12	5	15	5	74	31

[a] Error ± 5%
[b] BET equivalent primary particle diameter, calculated by 6 / SSA ρ. For ρ the mixed density was calculated according to the wt%.

Table 2. Primer design

Gene	*Forward primer*	*Reverse primer*
GAPDH	5' ATCAAGTGGGGCGATGCTGG 3'	5' CCATGACGAACATGGGGGCA 3'
OC	5' ACCATGAGAGCCCTCACACTCCT 3'	5' GTCTCTTCACTACCTCGCTGCC 3'
Runx2	5' TTACCCCTCCTACCTGAGCCAG 3'	5' TTCTGAAGCACCTGAAATGCGC 3'
Col-1	5' TGTTCAGCTTTGTGGACCTCCG 3'	5' CTGAGGCCGTTCTGTACGCA 3'
VEGF	5' AGGAGGAGGGCAGAATCATCA 3'	5' CTCGATTGGATGGCAGTAGCT 3'

Figure captions:

Figure 1. TEM image of the 13-93-5Sr bioactive glass nanoparticles.

Figure 2. A) Inductively coupled plasma (ICP) analysis of Sr (µg/l) in pooled cell culture medium (of 6 independent samples/group) after 2 weeks. B) Cell metabolism measured by AlamarBlue assay after 2 weeks of cell culture. Results are given as mean ± SEM. *$p < 0.05$.

Figure 3. Light microscopy of hBMSCs after 14 days of culture showing increased cell growth in groups with a higher concentration of bioactive glass nanoparticles.

Figure 4. Quantitative real time RT-PCR analyses for osteocalcin (A), collagen type 1 (B), VEGF (C) and Runx2 (D) (expressed as gene expression related to control group, ΔΔCT-method). Shown are mean ± SEM. *$p < 0.05$.

Supplementary data. XRD spectra of BG13-93-0Sr and Sr-containing BG13-93 with different Sr content

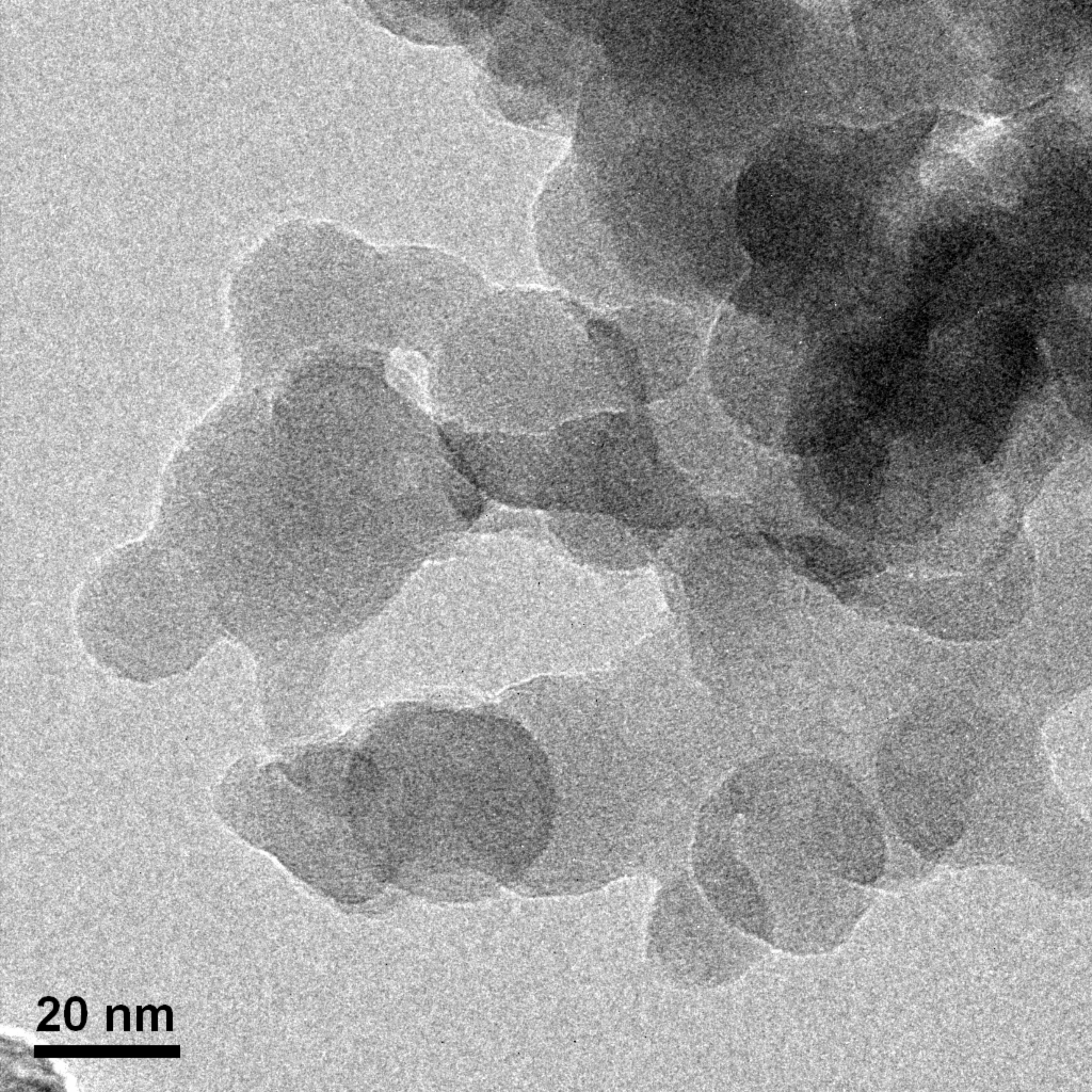
20 nm

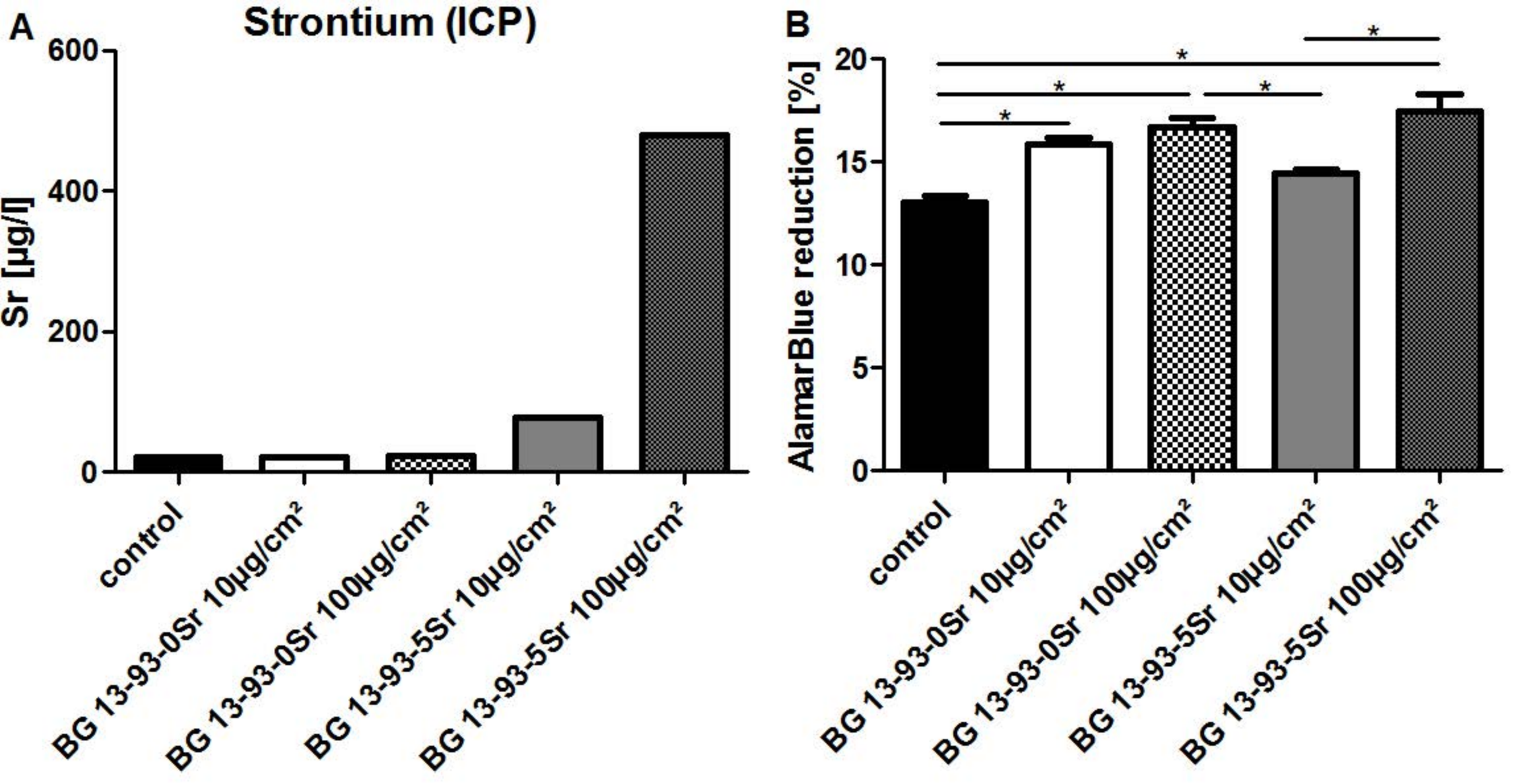
A
Strontium (ICP)
Sr [µg/l]
600
400
200
0
control
BG 13-93-0Sr 10µg/cm²
BG 13-93-0Sr 100µg/cm²
BG 13-93-5Sr 10µg/cm²
BG 13-93-5Sr 100µg/cm²
B
AlamarBlue reduction [%]
20
15
10
5
0
*
control
BG 13-93-0Sr 10µg/cm²
BG 13-93-0Sr 100µg/cm²
BG 13-93-5Sr 10µg/cm²
BG 13-93-5Sr 100µg/cm²

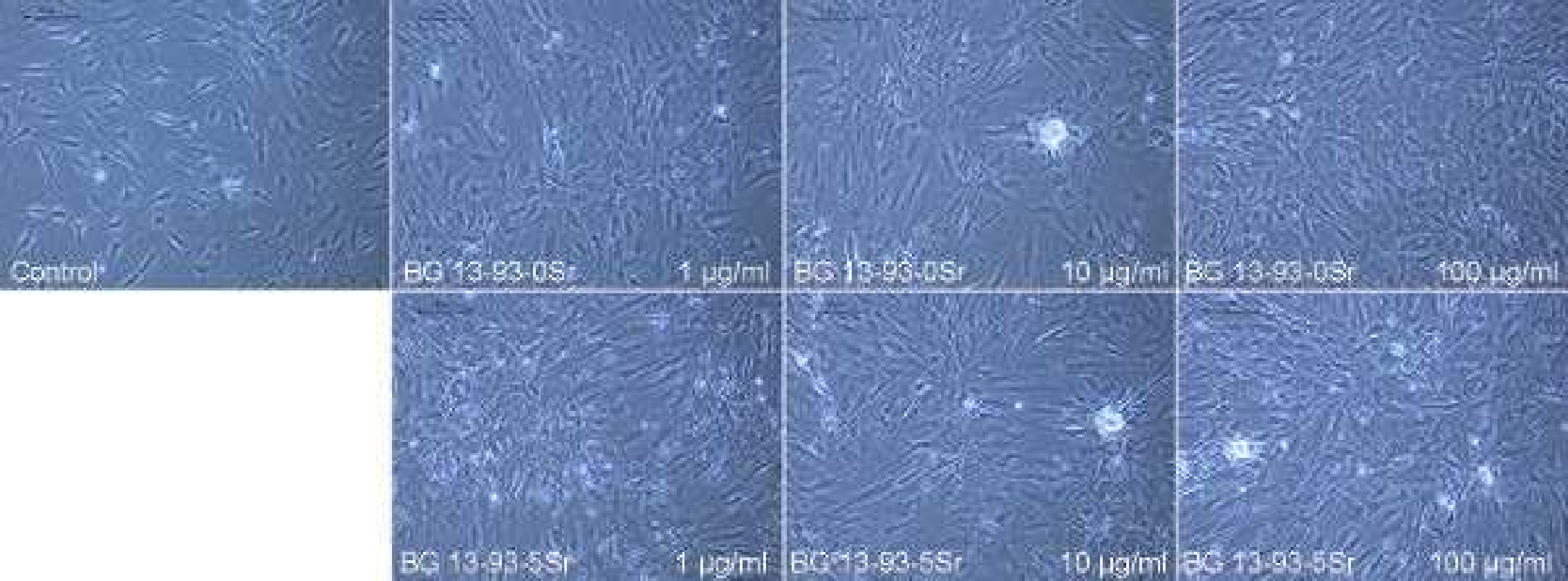
Control
BG 13-93-0Sr
1 µg/ml
BG 13-93-0Sr
10 µg/ml
BG 13-93-0Sr
100 µg/ml
BG 13-93-5Sr
1 µg/ml
BG 13-93-5Sr
10 µg/ml
BG 13-93-5Sr
100 µg/ml

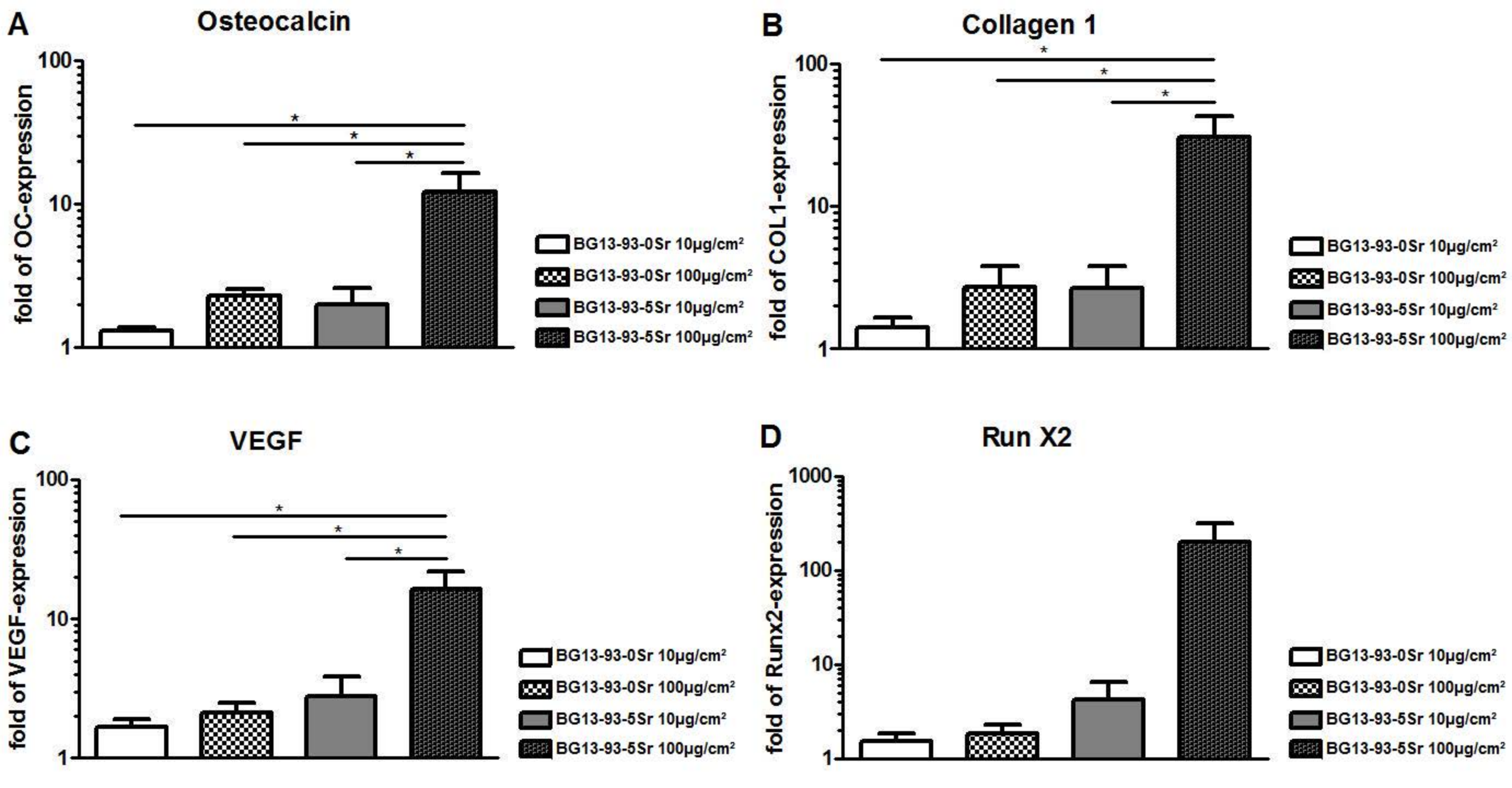
A
Osteocalcin
fold of OC-expression
100
10
1
*
*
*
BG13-93-0Sr 10μg/cm²
BG13-93-0Sr 100μg/cm²
BG13-93-5Sr 10μg/cm²
BG13-93-5Sr 100μg/cm²
B
Collagen 1
fold of COL1-expression
100
10
1
*
*
*
BG13-93-0Sr 10μg/cm²
BG13-93-0Sr 100μg/cm²
BG13-93-5Sr 10μg/cm²
BG13-93-5Sr 100μg/cm²
C
VEGF
fold of VEGF-expression
100
10
1
*
*
*
BG13-93-0Sr 10μg/cm²
BG13-93-0Sr 100μg/cm²
BG13-93-5Sr 10μg/cm²
BG13-93-5Sr 100μg/cm²
D
Run X2
fold of Runx2-expression
1000
100
10
1
BG13-93-0Sr 10μg/cm²
BG13-93-0Sr 100μg/cm²
BG13-93-5Sr 10μg/cm²
BG13-93-5Sr 100μg/cm²

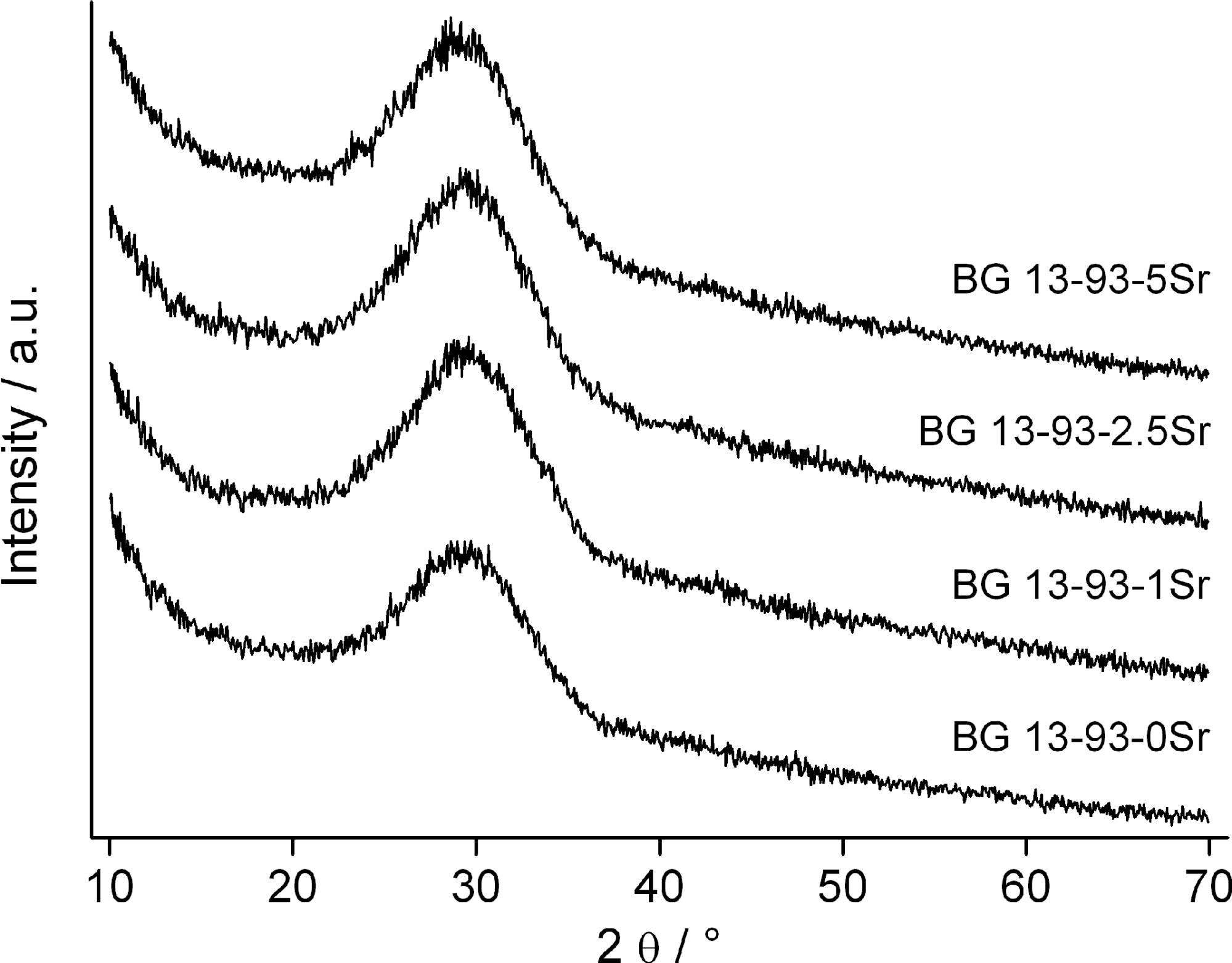
Intensity / a.u.
BG 13-93-5Sr
BG 13-93-2.5Sr
BG 13-93-1Sr
BG 13-93-0Sr
10
20
30
40
50
60
70
2 θ / °